Synthetic Metals 181 (2013) 98–103

Contents lists available at ScienceDirect

Synthetic Metals

journal homepage: www.elsevier.com/locate/synmet

Enhancement of external quantum efficiency through steric hindrance of phenazine derivative for white polymer light-emitting diode materials

Ho Jun Song[a], Eui Jin Lee[a], Doo Hun Kim[a], Seung Min Lee[a], Jang Yong Lee[b], Doo Kyung Moon[a,*]

[a] Department of Materials Chemistry and Engineering, Konkuk University, 1 Hwayang-dong, Gwangjin-gu, Seoul 143-701, Republic of Korea
[b] Energy Materials Research Center, Korea Research Institute of Chemical Technology, P.O. Box 107, Yuseong, Daejeon 305-600, Republic of Korea

ARTICLE INFO

Article history:
Received 17 June 2013
Received in revised form 16 August 2013
Accepted 22 August 2013
Available online 19 September 2013

Keywords:
Phenazine
Fluorene
Conjugated polymer
WPLED

ABSTRACT

Copolymers introducing dithienyl-benzophenazine (<0.1 mol%) as a dopant have been synthesized on a polyfluorene (PF) backbone based on the Suzuki coupling reaction. The UV–vis spectra of polymers showed similar behaviors in the solution and on the film. However, PL spectra were similar to that of PF in solution, but the peak around 615 nm increased as the amounts of dithienyl-benzophenazine were increased in the casting film. Compared with PF-PDTQ05, PF-FDTQ series showed red-shift emission peak by increased conjugation length of dithienyl-benzophenazine. The emission intensity of PF-FDTQ03 and PF-FDTQ05 was more intense compared to that of PF-PDTQ05 due to strong steric-hindrance of FDTQ. In case of PF-FDTQ05, the luminous efficiency and external quantum efficiency were 0.78 cd/A and 0.64%, respectively with a maximum brightness of 3112 cd/m^2.

1. Introduction

For the past decades, π-conjugated polymer has been applied to diverse applications such as organic light-emitting diodes (OLEDs) [1–6], organic photovoltaic cells (OPVs) [7–9], organic thin-film transistors (OTFTs) [10–12], and liquid crystal application (LC) [13]. In particular, polymer light-emitting diodes (PLED) present advantages in large-area fabrication methods, such as ink-jet and screen printing with solution processes. As a result, the material has drawn great attention as a next-generation material to replace vacuum deposition with small molecules. Thanks to its convenience and flexibility, polymer film has been popular in the flexible display sector [8,14].

A number of studies have been focusing on PLED materials in various colors since the development of poly(phenylenevinylene) in 1990 [15]. It has been reported that polyfluorene (PF) [16], poly(phenylenevinylene) (PPV) [17], and poly(methoxy, ethyl-hexyloxy phenylene vinylene) (MEH-PPV) [18] are the representative blue-emitting, green-emitting, and orange and red-emitting materials, respectively. Full-color displays have been enabled by such polymers [4,8].

Recently, there have been more studies on white polymer light-emitting diodes (WPLED) that introduced diverse chromophores to the blue emitting material, PF. If chromophore is introduced to a PF backbone, aggregation and excimers are suppressed. As a result, effective energy transfer occurs in such materials. Therefore, high-efficiency WPLEDs can be realized [19,20]. Recently, we introduced a small amount of low-band-gap chromophore (<0.3 mol%) to a PF backbone and had it copolymerized. Depending on the dopant mol ratio, various color changes (white, green, yellow, etc.) could be detected with high efficiency [5].

The electron-deficient quinoxaline derivative is a leading orange-emitting chromophore. Due to thermal and electrochemical stability and high PL and EL efficiency, the quinoxaline derivative has been widely used in white and orange light-emitting polymers [21–23]. In addition, the quinoxaline derivative can be easily tuned in structure with high solubility. Therefore, electronic characteristics can be changed by introducing various substituents [24,25].

Recently, the various group reported that with the two phenyl rings connected to the single bond between ortho-positions of quinoxaline derivative [26–28]. These fused-phenyl rings can enhance the quantum efficiency through steric hindrance between fused quinoxaline and adjacent derivative and improve interchain π–π interactions among polymer backbones [29,30].

In this study, 0.03–0.1 mol% of phenazine derivative was adopted as dopant with an orange emitter and PF as a host. The

* Corresponding author. Tel.: +82 2 450 3498; fax: +82 2 444 0765.
E-mail address: dkmoon@konkuk.ac.kr (D.K. Moon).

0379-6779/$ – see front matter © 2013 Elsevier B.V. All rights reserved.
http://dx.doi.org/10.1016/j.synthmet.2013.08.017

Forster energy transfer was investigated, as well as the charge trapping and quantum efficiency between host and dopant, and the optimum mol concentration for effective white-emitting polymer was realized.

2. Experiment

2.1. Instruments and characterization

Unless otherwise specified, all the reactions were carried out under nitrogen atmosphere. Solvents were dried by standard procedures. Column chromatography was performed with the use of silica gel (230–400 mesh, Merck) as the stationary phase. ^{1}H NMR spectra were performed in a Bruker ARX 400 spectrometer using solutions in $CDCl_3$, and chemical concentrations were recorded in units of ppm with TMS as the internal standard. Electronic absorption spectra were measured in chloroform using a HP Agilent 8453 UV–Vis spectrophotometer. Photoluminescent spectra were recorded by a Perkin Elmer LS 55 luminescence spectrometer. Cyclic voltammetry experiments were performed with a Zahner IM6eX Potentionstat/Galvanostat. All measurements were carried out at room temperature with a conventional three-electrode configuration consisting of platinum working and auxiliary electrodes and a nonaqueous Ag/AgCl reference electrode at the scan rate of 50 mV/s. The solvent in all experiments was acetonitrile and the supporting electrolyte was 0.1 M tetrabutyl ammonium-tetrafluoroborate. TGA measurements were performed on a NETZSCH TG 209 F3 thermogravimetric analyzer. All GPC analyses were made by using THF as the eluant and polystyrene standard as the reference. Theoretical study was performed by using density functional theory (DFT), as approximated by the B3LYP functional and employing the 6-31G* basis set in Gaussian09.

2.2. EL device fabrication and characterization

The fabricated device structure was ITO/PEDOT:PSS/polymer/BaF_2/Ba/Al. All of the polymer light-emitting diodes were prepared using the following device fabrication procedure. Glass/indium tin oxide (ITO) substrates [Sanyo, Japan (10 Ω/γ)] were sequentially patterned lithographically, cleaned with detergent, and ultrasonicated in deionized water, acetone and isopropyl alcohol. Then, the substrates were dried on a hotplate at 120 °C for 10 min and treated with oxygen plasma for 10 min in order to improve the contact angle just before the film coating process. Poly(3,4-ethylenedioxythiophene): poly(styrene-sulfonate) (PEDOT:PSS, Baytron P 4083 Bayer AG) was passed through a 0.45-μm filter before being deposited onto ITO at a thickness of ca. 32 nm through spin-coating at 4000 rpm in air, and then dried at 120 °C for 20 min inside a glove box. The light-emitting polymer layer was then deposited onto the film by spin coating a polymer solution in chlorobenzene (1.5 wt.%) at a speed of 1000 rpm for 30 s on top of the PEDOT:PSS layer. The device was thermally annealed at 90 °CC for 30 min in a glove box. The device fabrication was completed by depositing thin layers of BaF_2 (1 nm), Ba (2 nm) and Al (200 nm) at pressures less than 10^{-6} Torr. The active area of the device was 9.0 mm^2. Finally, the cell was encapsulated using UV-curing glue (Nagase, Japan). EL spectra, Commission Internationale de l'Eclairage (CIE) coordinates, current–voltage, and brightness–voltage characteristics of devices were measured with a Spectrascan PR670 spectrophotometer in the forward direction, and a computer-controlled Keithley 2400 under ambient conditions.

2.3. Materials and synthesis of monomers

All reagents were purchased from Aldrich, Acros or TCI companies. All chemicals were used without further purification. The following compounds were synthesized following modified literature procedures: 10,13-bis(5-bromothiophen-2-yl)-11,12-bis(octyloxy)dibenzo [a,c]phenazine **M1** [29], 5,8-bis(5-bromothiophen-2-yl)-2,3-bis(4-(hexyloxy) phenyl)quinoxaline **M2**, 2,2′-(9,9-dioctyl-9H-fluorene-2,7-diyl)bis(4,4,5,5-tetramethyl-1,3,2-dioxaborolane) **M3** [31].

2.4. Polymerization

Reaction monomers $(PPh_3)_4Pd(0)$ (1.5 mol%) and Aliquat 336 were dissolved in a mixture of toluene and an aqueous solution of 2 M K_2CO_3. The solution was refluxed for 72 h with vigorous stirring in nitrogen atmosphere, and then excess amounts of bromobenzene, as an end capper, were added and stirring continued for 12 h. The whole mixture was poured into methanol. The precipitate was filtered off, and purified with methanol, acetone, hexane, chloroform in soxhlet.

PF-FDTQ03. 9,9-dioctylfluorene-2,7-dibromofluorene (0.499 equiv), 2,2′-(9,9-dioctyl-9H-fluorene-2,7-diyl)bis(4,4,5,5-tetramethyl-1,3,2-dioxaborolane) (**M3**) (0.5 equiv), 10,13-bis(5-bromothiophen-2-yl)-11,12-bis(octyloxy)dibenzo [a,c]phenazine (**M1**) (0.0003 equiv); Yield: 0.33 g (76%); ^{1}H NMR (400 MHz; $CDCl_3$; Me_4Si): δ = 7.85-7.75 (m), 7.71-7.67 (m), 7.62-7.33 (m), 2.11 (br), 1.28-1.13 (m), 0.98-0.79 (m).

PF-FDTQ05. 9,9-dioctylfluorene-2,7-dibromofluorene (0.499 equiv), 2,2′-(9,9-dioctyl-9H-fluorene-2,7-diyl)bis(4,4,5,5-tetramethyl-1,3,2-dioxaborolane) (**M3**) (0.5 equiv), 10,13-bis(5-bromothiophen-2-yl)-11,12-bis(octyloxy)dibenzo [a,c]phenazine (**M1**) (0.0005 equiv); Yield: 0.32 g (74%); ^{1}H NMR (400 MHz; $CDCl_3$; Me_4Si): δ = 7.85-7.75 (m), 7.71-7.67 (m), 7.62-7.33 (m), 2.11 (br), 1.28-1.13 (m), 0.98-0.79 (m).

PF-FDTQ10. 9,9-dioctylfluorene-2,7-dibromofluorene (0.499 equiv), 2,2′-(9,9-dioctyl-9H-fluorene-2,7-diyl)bis(4,4,5,5-tetramethyl-1,3,2-dioxaborolane) (**M3**) (0.5 equiv), 10,13-bis(5-bromothiophen-2-yl)-11,12-bis(octyloxy)dibenzo [a,c]phenazine (**M1**) (0.001 equiv); Yield: 0.32 g (74%); ^{1}H NMR (400 MHz; $CDCl_3$; Me_4Si): δ = 7.85-7.75 (m), 7.71-7.67 (m), 7.62-7.33 (m), 2.11 (br), 1.28-1.13 (m), 0.98-0.79 (m).

PF-PDTQ05. 9,9-dioctylfluorene-2,7-dibromofluorene (0.499 equiv), 2,2′-(9,9-dioctyl-9H-fluorene-2,7-diyl)bis(4,4,5,5-tetramethyl-1,3,2-dioxaborolane) (**M3**) (0.5 equiv), 5,8-bis(5-bromothiophen-2-yl)-2,3-bis(4-(hexyloxy)phenyl)quinoxaline (**M2**) (0.0005 equiv); Yield: 0.31 g (72%); ^{1}H NMR (400 MHz; $CDCl_3$; Me_4Si): δ = 7.85-7.75 (m), 7.71-7.67 (m), 7.62-7.33 (m), 2.11 (br), 1.28-1.13 (m), 0.98-0.79 (m).

3. Results and discussion

3.1. Synthesis and characterization of the polymers

As shown in Scheme 1, a total of 4 polymers were polymerized through Suzuki coupling reaction by using different mol ratios (monomers a, b and c) with 72–76% yield ratio. The polymerization was reacted at 90 °C for 72 h with palladium catalyst (0) and 2 M potassium carbonate solution. In addition, aliquot 336 and toluene were used as surfactant and solvent, respectively. Once the polymerization was completed, it was end-capped with bromobenzene. All polymers were purified with soxhlet in order of methanol, acetone and chloroform, and the chloroform fraction was recovered. All polymers dissolved in general organic solvents such as THF, chloroform, chlorobenzene and dichlorobenze, and

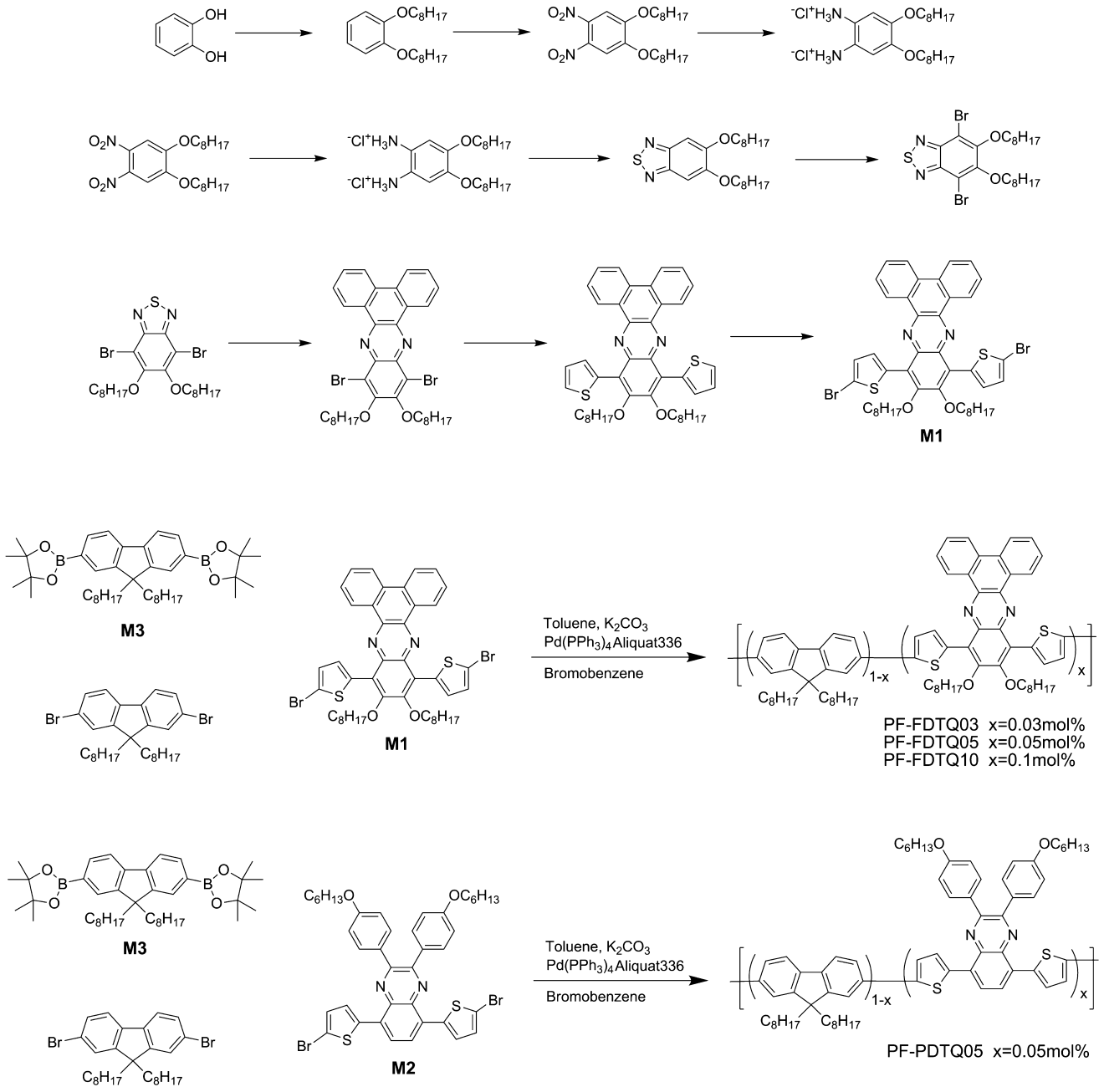

Scheme 1. Monomer synthesis and polymerization.

a homogenous and transparent film has been formed through spin-coating.

In the H NMR spectra obtained (see Fig. S1), an aromatic peak was found at 7.0–8.0 ppm, while a proton peak originating from an aliphatic peak was detected at 0.8–5.0 ppm. A proton peak from the small amount (10^{-4} mol against total monomer) of the dithienylbenzophenazine (M1) dopant was not observed. As shown in the references, the actual dopant ratio could not be measured through NMR, FT-IR or elemental analysis against the dopant ratio 0.5 mol% or below [5,32]. As shown in Table 1, according to the measurement of GPC with polystyrene as the standard, the number average molecular weight of all polymers ranged from 15.8 to 17.0 kg/mol. The degree of polymerization was similar to that of general EL polymer [5]. The polydispersity indices (PDI) showed a very narrow distribution (1.93–2.13).

Thermal analysis through TGA (see Fig. S2) showed high thermal stability (around 400°) at 5 wt.% loss, which reveals applicability to display application sectors in which high thermal stability (400 °C or higher) is required [5,31]. In addition, thermal characteristics

Table 1
Physical properties of the polymers.

Polymer	M_n (kg/mol)	M_w (kg/mol)	PDI	T_d (°C)[a]	Φ_{PL}[b]
PF	17.5	32.3	1.84	416	0.79
PF-FDTQ03	15.8	31.5	1.99	412	0.79
PF-FDTQ05	16.1	31.5	1.95	412	0.77
PF-FDTQ10	16.7	35.6	2.13	412	0.78
PF-PDTQ05	17.0	32.3	1.84	409	0.79

[a] Temperature resulting in 5% weight loss based on initial weight.
[b] Solution fluorescence quantum yields measured in chloroform relative to polyfluorene (ca. 1×10^{-5} M, $\Phi_{PL} = 0.79$) in chloroform as a standard.

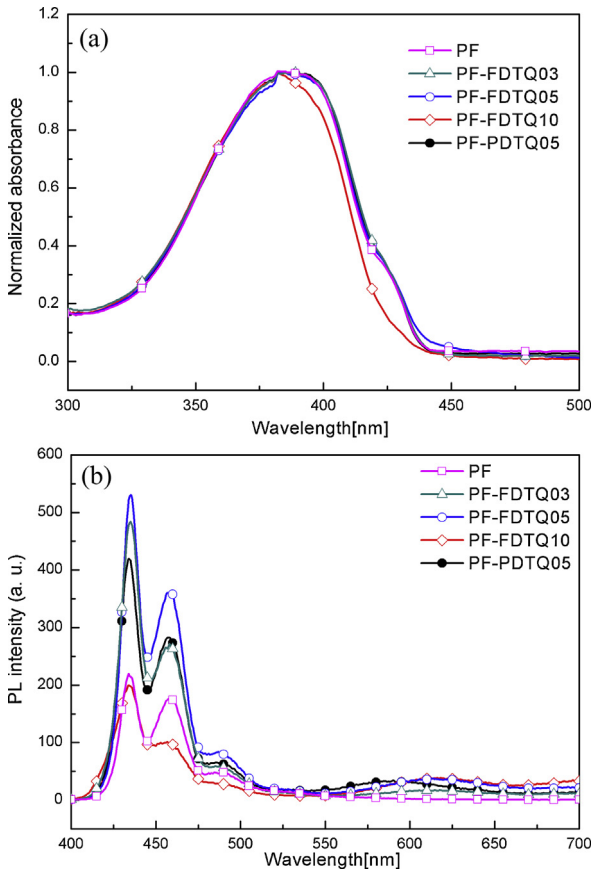

Fig. 1. (a) UV–vis absorption spectra and (b) PL emission spectra in thin film (thickness: 70–80 nm) of polymers.

similar to PF were found in all polymers, which means that the dopant introduced to the PF backbone had no effect on polymer rigidity. The weight loss of 45–50% at 400–500 °C is the result of the degradation of the skeletal PF backbone chain structure. The PF backbone is decomposed to oligomers or other short chain structures [33].

3.2. Optical and electrochemical properties

Fig. 1 shows the UV–visible spectra and PL spectra of all polymer films. As shown in Fig. 1(a), for film state, the absorption spectra of all polymers was broad in comparison with those of the solution (see Fig. S3(a)). This kind of result was because the dihedral angle between fluorene rings in the thin film is considered to decrease due to stronger interchain interaction [32,34,35]. The absorption peak of the M1 and M2 (dopant) was not observed because of the small amount of dopant used.

In case of PL spectra, as shown in Fig. 1(b), as M1 content increased, the 615 nm emission peak broadened, unlike for the solution, because of increases in the intermolecular interaction among the polymer main chains [19]. In addition, PF-FDTQ series polymers showed the red-shift phenomenon for dopant emission region compared with PF-PDTQ (λ_{max} = 590 nm), which is the result of increased conjugation length by rigid structure of M1 compared to M2 (see Fig. 2(a)). Interestingly, the emission intensity of PF-FDTQ03 and PF-FDTQ05 were more intense compared to that of PF-PDTQ05, which was caused by strong steric-hindrance of M1 compared to that of M2 (see Fig. 2(b)). This result might be expected to show effective quantum efficiency.

According to the comparison between the UV–vis spectra of M1, M2 and PL spectra of PF (see Fig. S4), the absorption spectra of

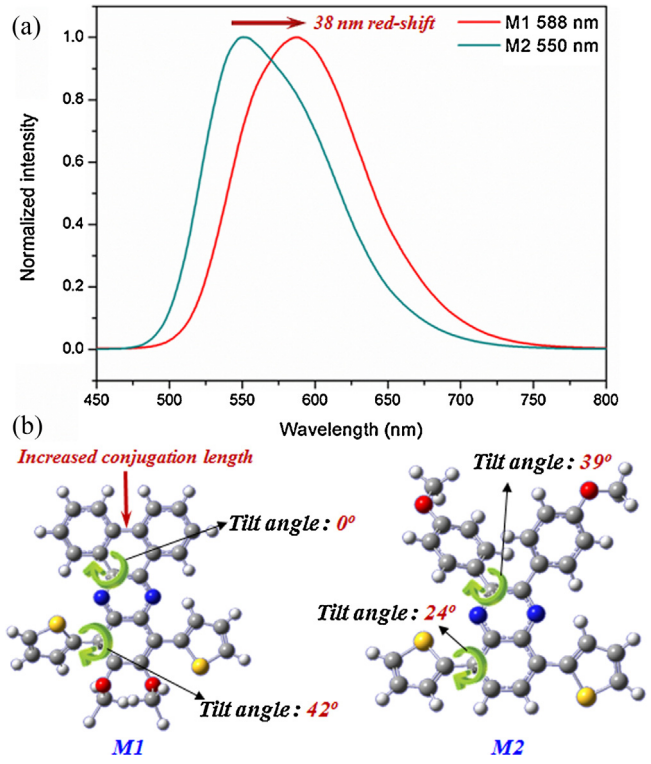

Fig. 2. (a) PL emission spectra and (b) torsion angle of M1, M2 through DFT Gaussian simulation.

M1, M2 derivative were overlapped in the PL spectra of PF, which means effective absorption of PF emission energy by M1, M2. Therefore, effective Forster energy transfer from PF backbone to M1, M2 derivative would occur in the copolymer.

Fig. 3 showed the electrochemical properties of the polymers which were measured through cyclic voltammetry (CV). The highest occupied molecular orbital (HOMO) levels of polymers were calculated using the oxidation onset value of polymers and the reference energy level (4.8 eV below the vacuum level) of ferrocene as follows:

$$\text{HOMO (eV)} = -4.8 - (E_{\text{onset}} - E_{1/2}\ \text{(Ferrocene)}) \quad (1)$$

In contrast, the lowest unoccupied molecular orbital (LUMO) levels were estimated based on the difference between the HOMO

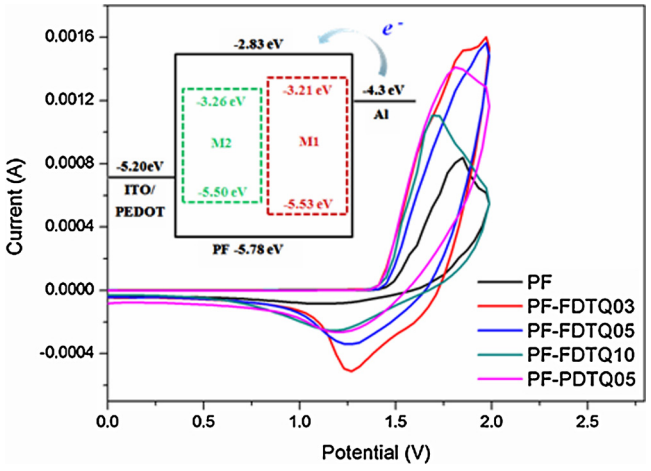

Fig. 3. Cyclic voltammograms of polymers and band diagram of PF, M1 and M2 (inset).

Table 2
Optical and electrochemical properties of polymers.

Polymer	Solution, λ_{max} (nm)		Film, λ_{max} (nm)		E_{HOMO} (eV)	E_{LUMO} (eV)
	Absorption	Emission	Absorption	Emission		
PF	388	417, 439	382	434, 458	5.77	2.95
PF-FDTQ03	388	417, 439	387	435, 458, 614	5.80	2.98
PF-FDTQ05	388	417, 439	387	435, 458, 613	5.83	3.03
PF-FDTQ10	388	417, 439	387	434, 457, 616	5.85	3.02
PF-PDTQ03	388	417, 439	387	432, 586, 590	5.83	3.01

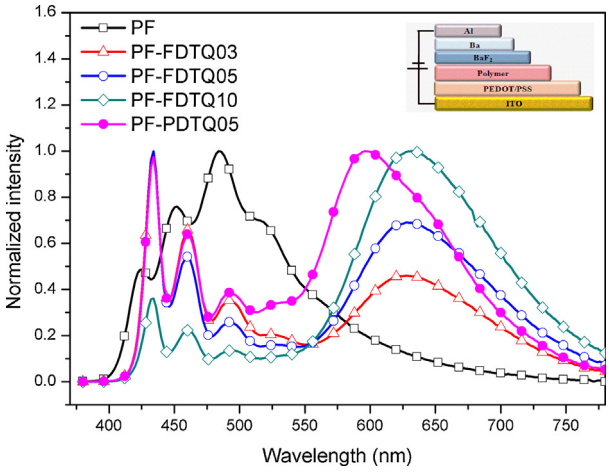

Fig. 4. EL luminescence spectra of polymers.

level and the optical band gap calculated from UV–vis absorption onset value of polymer thin film. The HOMO and LUMO levels of the polymers and optical band gap are exhibited in Table 2.

The HOMO levels of all polymers were −5.80 to −5.85 eV and the LUMO levels were −2.98 to −3.03 eV, respectively. In terms of the HOMO and LUMO levels, all polymers were similar with PF, because the M1, M2 dopant content was very small (0.1 mol% or less), having little effect on the polymer backbone [5]. The inset in Fig. 3 shows the energy band diagrams of PF, M1 and M2 derivative. As shown in these diagrams, the energy level of the M1, M2 dopant exists between the HOMO and LUMO levels of PF. Thus, it was expected that charge trapping would effectively occur from PF to M1, M2 [5,35].

3.3. Electroluminescence properties and current–voltage–luminance characteristics

Fig. 4 shows the electroluminescent spectra of the EL device. The brightness–voltage and efficiency–current density of the EL device are shown in Fig. 5(a) and (b), respectively, and their characteristics are summarized in Table 3. The device was fabricated with ITO/PEDOT:PSS/polymer/BaF_2/Ba/Al structure, as shown in the inset of Fig. 4, and the emission layer was fabricated to 70–80 nm thickness through spin-coating. In case of PF-FDTQ03, PF-FDTQ05 and PF-FDTQ10, emissions broadened at 550–700 nm as the M1 derivative content increased, because of incomplete energy

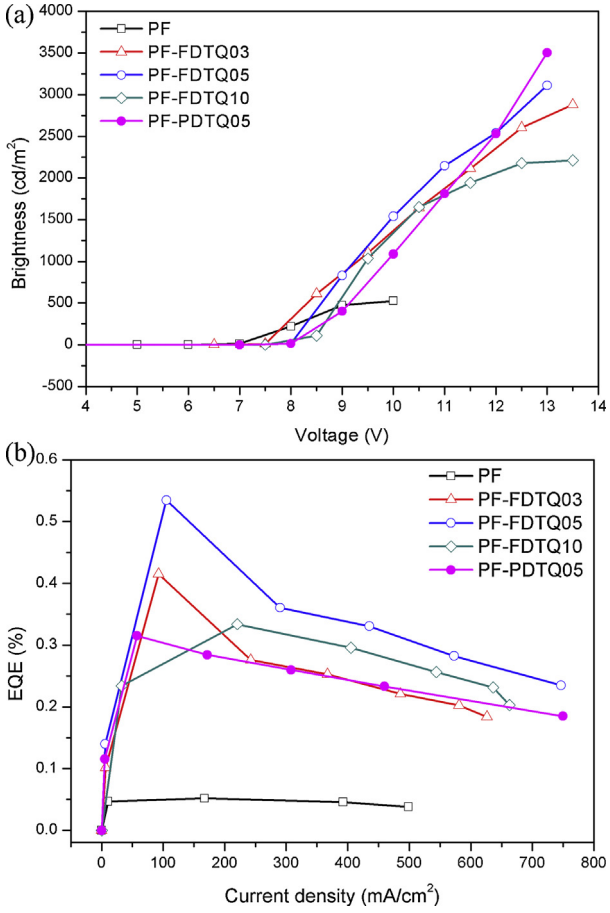

Fig. 5. (a) voltage–luminance (*V*–*L*), (b) current density–external quantum efficiency (*J*–EQE) curve.

transfer from fluorene derivative to M1 derivative. Furthermore, as M1 derivative content increased, spectra intensity increased at 630 nm with similar pattern to the PL spectra. In case of PF-PDTQ05, on the other hand, emissions broadened at 550–670 nm with λ_{max} = 596 nm. The EL spectra of PF-FDTQ series showed the red-shift phenomenon compared with that of PF-PDTQ, which is due to red-shifted emission of M1 by increased conjugation length compared to emission of M2.

Overall, differences were found between the PL spectra and EL spectra. Unlike in the PL spectra, similar intensity was found in

Table 3
Summary of EL device performances of polymers.

Polymer	EL emission λ_{max} (nm)	Luminous efficiency (cd/A)	External quantum efficiency (%)	Maximum brightness (cd/m^2)	CIE coordinate (x, y)
PF	424, 484	0.13	0.05	527	(0.21, 0.29)
PF-FDTQ03	434, 628	0.66	0.41	2880	(0.32, 0.23)
PF-FDTQ05	434, 628	0.78	0.53	3112	(0.38, 0.25)
PF-FDTQ10	434, 632	0.46	0.33	2212	(0.48, 0.31)
PF-PDTQ05	434, 596	0.70	0.31	3502	(0.40, 0.32)

orange–red emissions (λ_{max} = 596, 628 nm) in the blue emission (λ_{max} = 432 nm) of the EL spectra. It has been confirmed that the low energy level of M1, M2 derivative worked as a charge trapping site. This kind of result is matched with the HOMO and LUMO levels of the dopant confirmed in electrochemical measurements [5,19]. As shown in Table 3, the CIE coordinates of PF-FDTQ05 and PF-PDTQ05 were (0.38, 0.25) and (0.40, 0.32), respectively, which are close to the pure white coordinates of (0.33, 0.33).

The best EL performance was exhibited in PF-FDTQ05, which was observed with 0.78 cd/A luminous efficiency, 0.53% external quantum efficiency (EQE), 3112 cd/m^2 maximum brightness, and CIE coordinates of (0.38, 0.25). Stable luminous efficiency and the best performance occurred in PF-FDTQ05 because of the well-balanced electron and hole injection in the M1 derivative ratio and effective energy transfer and charge trapping between fluorene and M1 derivative [5,35]. In terms of EL performance, EQE of PF-FDTQ05 showed improvement of 1.7 times compared to that of PF-PDTQ05, which might be because M1 have high quantum efficiency by steric-hindrance. The EL performance of PF-FDTQ10 was relatively poorer than that of other polymers because the M1 derivative worked as a charge trapping site along the polymer backbone and exhibited exciton quenching [19].

4. Conclusions

We successfully synthesized white-emitting polymers containing phenazine and quinoxaline on a PF backbone. The synthesized polymers showed good solubility and thermal stability. In case of PL spectra, as phenazine derivative (M1) content increased, the 615 nm emission peak broadened compared with quinoxline derivative (M2, 590 nm) because of increased conjugation length by rigid structure of M1. Interestingly, the emission intensity of PF-FDTQ03 and PF-FDTQ05 were more intense compared to that of PF-PDTQ05, which was caused by strong steric-hindrance of M1 compared to that of M2. In terms of EL performance, EQE of PF-FDTQ05 showed improvement of 1.7 times compared to that of PF-PDTQ05, which might be because M1 have high quantum efficiency by steric-hindrance. The luminous efficiency, maximum brightness, and CIE coordinates of the device were 0.78 cd/A, 0.53% external quantum efficiency, 3112 cd/m^2, and (0.38, 0.25), close to white emission, respectively.

Acknowledgment

This work was supported by the technology supporting project grant funded by the Korea government Ministry of Knowledge Economy (No. 2012K10042360).

Appendix A. Supplementary data

Supplementary data associated with this article can be found, in the online version, at http://dx.doi.org/10.1016/j.synthmet.2013.08.017.

References

[1] R.H. Friend, R.W. Gymer, A.B. Holmes, J.H. Burroughes, R.N. Marks, C. Taliani, D.D.C. Bradley, D.A. Dos Santos, J.L. Bredas, M. Logdlund, W.R. Salaneck, Nature 397 (1999) 121–128.
[2] C. Ulbricht, B. Beyer, C. Friebe, A. Winter, U.S. Schubert, Adv. Mater. 21 (2009) 4418–4441.
[3] H.J. Song, J.Y. Lee, I.S. Song, D.K. Moon, J.R. Haw, J. Ind. Eng. Chem. 17 (2011) 352–357.
[4] M. Kijima, I. Kinoshita, T. Hattori, H. Shirakawa, Synth. Met. 100 (1999) 61–69.
[5] H.J. Song, D.H. Kim, T.H. Lee, D.K. Moon, Eur. Polym. J. 48 (2012) 1485–1494.
[6] H. Wu, L. Ying, W. Yang, Y. Cao, Chem. Soc. Rev. 38 (2009) 3391–3400.
[7] A. Gadisa, W. Mammo, L.M. Andersson, S. Admassie, F. Zhang, L. Chen, M.R. Andersson, O. Inganäs, Adv. Funct. Mater. 23 (2007) 3836–3842.
[8] E. Wang, L. Hou, Z. Wang, S. Hellström, F. Zhang, O. Inganäs, M.R. Andersson, Adv. Mater. 22 (2010) 5240–5244.
[9] J.Y. Lee, S.H. Kim, I.S. Song, D.K. Moon, J. Mater. Chem. 21 (2011) 16480–16487.
[10] J.Y. Lee, A.N. Aleshin, D.W. Kim, H.J. Lee, Y.S. Kim, G. Wegner, V. Enkelmann, S. Roth, Y.W. Park, Synth. Met. 152 (2005) 169–172.
[11] I. Mcculloch, M. Heeney, C. Bailey, K. Genevicius, I. Macdonald, M. Shkunov, D. Sparrowe, S. Tierney, R. Wagner, W. Zhang, M.L. Chabinyc, R.J. Kline, M.D. Mcgehee, M.F. Toney, Nat. Mater. 5 (2006) 328–333.
[12] I. Osaka, M. Shimawaki, H. Mori, I. Doi, E. Miyazaki, T. Koganezawa, K. Takimiya, J. Am. Chem. Soc. 134 (2012) 3498–3507.
[13] M. Goh, S. Matsushita, K. Akagi, Chem. Soc. Rev. 39 (2010) 2466–2476.
[14] M.M. Alam, S.A. Jenekhe, Chem. Mater. 14 (2002) 4775–4780.
[15] J.H. Burroughes, D.D.C. Bradley, A.R. Brown, R.N. Marks, K. Mackay, R.H. Friend, P.L. Burns, A.B. Holmes, Nature 347 (1990) 539–541.
[16] Q. Pei, Y. Yang, J. Am. Chem. Soc. 118 (1996) 7416–7417.
[17] Z. Tan, R. Tang, E. Zhou, Y. He, C. Yang, F. Xi, Y. Li, J. Appl. Polym. Sci. 107 (2008) 514–521.
[18] X.Y. Deng, W.M. Lau, K.Y. Wong, K.H. Low, H.F. Chow, Y. Cao, Appl. Phys. Lett. 84 (2004) 3522–3524.
[19] M.J. Park, J.H. Lee, I.H. Jung, J.H. Park, D.H. Hwang, H.K. Shim, Macromolecules 41 (2008) 9643–9649.
[20] Q. Hou, Y. Xu, W. Yang, M. Yuan, J. Peng, Y. Cao, J. Mater. Chem. 12 (2002) 2887–2892.
[21] M. Sun, Q. Niu, B. Du, J. Peng, W. Yang, Y. Cao, Macromol. Chem. Phys. 208 (2007) 988–993.
[22] E. Xu, H. Zhong, H. Lai, D. Zeng, J. Zhang, W. Zhu, Q. Fang, Macromol. Chem. Phys. 211 (2010) 651–656.
[23] A. Tsami, X.H. Yang, F. Galbrecht, T. Farrell, H. Li, S. Adamczyk, R. Heiderhoff, L.J. Balk, D. Neher, E. Holder, J. Polym. Sci. A: Polym. Chem. 45 (2007) 4773–4785.
[24] Y.K. Lee, Y.M. Nam, W.H. Jo, J. Mater. Chem. 21 (2011) 8583–8590.
[25] N. Blouin, A. Michaud, D. Gendron, S. Wakim, E. Blair, R. Neagu-Plesu, M. Belletete, G. Durocher, Y. Tao, M. Leclerc, J. Am. Chem. Soc. 130 (2008) 732–742.
[26] R. Mondal, S. Ko, E. Verploegen, H.A. Becerril, M.F. Toney, Z. Bao, J. Mater. Chem. 21 (2011) 1537–1543.
[27] Y. Zhang, J. Zou, H.-L. Yip, K.-S. Chen, J.A. Davies, Y. Sun, A.K.Y. Jen, Macromolecules 44 (2011) 4752–4758.
[28] Y. Zhang, J. Zou, H.-L. Yip, K.-S. Chen, D.F. Zeigler, Y. Sun, A.K.Y. Jen, Chem. Mater. 23 (2011) 2289–2291.
[29] H.J. Song, T.H. Lee, M.H. Han, J.Y. Lee, D.K. Moon, Polymer 54 (2013) 1072–1079.
[30] Y.H. Kim, S.J. Lee, S.Y. Jung, K.N. Byeon, J.S. Kim, S.C. Shin, S.K. Kwon, Bull. Kor. Chem. Soc. 28 (2007) 443–446.
[31] M.H. Han, H.J. Song, T.H. Lee, J.Y. Lee, D.K. Moon, J.R. Haw, Synth. Met. 162 (2012) 2294–2301.
[32] B.-Y. Hsieh, Y. Chen, J. Polym. Sci. A: Polym. Chem. 47 (2009) 833–844.
[33] J. Xu, Y. Zhang, J. Hou, Z. Wei, S. Pu, J. Zhao, Y. Du, Eur. Polym. J. 42 (2006) 1154–1163.
[34] M. Fukuda, K. Sawada, K. Yoshino, J. Polym. Sci. A: Polym. Chem. 31 (1993) 2465–2471.
[35] Q. Chen, N. Liu, L. Ying, W. Yang, H. Wu, W. Xu, Y. Cao, Polymer 50 (2009) 1430–1437.